A posteriori error estimates and adaptive finite elements for a nonlinear parabolic problem related to solidification

Olivier Krüger, Marco Picasso, Jean-Francois Scheid

A posteriori error estimates and adaptive finite elements for a nonlinear parabolic problem related to solidification

O. Krüger [a,1], M. Picasso [a] and J.-F. Scheid [a,b,1]

[a] *Département de Mathématiques, Ecole Polytechnique Fédérale de Lausanne, 1015 Lausanne, Switzerland*

[b] *Université Henri Poincaré Nancy 1, Institut Elie Cartan, B.P. 239, 54506 Vandoeuvre-les-Nancy Cedex, France*

Abstract

A posteriori error estimates are derived for a nonlinear parabolic problem arising from the isothermal solidification of a binary alloy. Space discretization with continuous, piecewise linear finite elements is considered. The L^2 in time H^1 in space error is bounded above and below by an error estimator based on the equation residual. Numerical results show that the effectivity index is close to one. An adaptive finite element algorithm is proposed and a solutal dendrite is computed.

1 Introduction

A posteriori error estimates are at the base of adaptive finite elements for a great number of problems. The goal is to provide an estimation of the true error and to adapt the mesh according to this error estimation. The estimated error is said to be equivalent to the true error if

$$c \leq \frac{\text{true error}}{\text{estimated error}} \leq C,$$

where the constants c and C depend only on the shape of the mesh triangles. An important point to control the quality of the error estimator is to consider

[1] Supported by the Swiss National Science Foundation.

the effectivity index defined by

$$\text{eff} = \frac{\text{estimated error}}{\text{true error}}.$$

This subject has been initiated in [1,2] and extended to linear elliptic problems, see for instance [3–8], and to nonlinear elliptic problems [9–12].

Several a posteriori error estimates have been derived for parabolic problems. In [13,14] a posteriori error estimates are derived for linear and nonlinear parabolic problems when using the discontinuous Galerkin method. The L^∞ in time, L^2 in space error is bounded above by an explicit error estimator using sharp a priori estimates for the dual problem. These a posteriori estimates are optimal in the sense that they are bounded above by a priori error estimates and numerical results are included. In [15] a general framework is developed for nonlinear evolution equations and a posteriori error estimates are derived in the L^∞ in time, L^2 in space error. Several examples are considered such as the Stefan problem (see also [16] for numerical results) or reaction -diffusion equations. In [17,18], the general framework introduced in [12] is extended to a wide class of nonlinear parabolic problems. Quasilinear parabolic equations of second order, the time-dependent incompressible Navier-Stokes equations are considered. A posteriori error estimates are obtained for several norms, upper and lower bounds are proposed. In [19], a theoretical and numerical study of the effectivity index is proposed for the linear heat equation. The L^2 in time, H^1 in space error is bounded above and below by an explicit error estimator based on the equation residual. Numerical results show that the effectivity index is close to one when using an adaptive algorithm. Finally, a general study of the effectivity index for linear parabolic equations is developped in [20,21]. Different strategies, namely h, p and r refinement are discussed, error estimators are proposed for p odd or even. Numerical results show that the method is still reliable for a nonlinear reaction-diffusion problem.

The goal of this paper is to extend some of the results obtained in [19] to a nonlinear parabolic problem arising from isothermal solidification of a binary alloy. More precisely, we consider the phase-field model proposed in [22] and presented hereafter. Given a domain Ω of $\mathbb{R}^2$ (with outer unit normal $\mathbf{n}$) and a final time T, the problem consists in finding the order parameter ϕ and the concentration c such that

$$\frac{\partial \phi}{\partial t} - \varepsilon^2 \Delta \phi = F_1(\phi) + cF_2(\phi) \qquad \text{in } \Omega \times (0,T), \tag{1}$$

$$\frac{\partial c}{\partial t} - D_1 \Delta c - \text{div } (D_2(c,\phi)\nabla \phi) = 0 \qquad \text{in } \Omega \times (0,T), \tag{2}$$

$$\nabla \phi \cdot \mathbf{n} = \nabla c \cdot \mathbf{n} = 0 \qquad \text{on } \partial\Omega \times (0,T), \tag{3}$$

$$\phi(0) = \phi_0 \quad c(0) = c_0 \qquad \text{in } \Omega. \tag{4}$$

Here ε and $D_1 > 0$ are given parameters, F_1, F_2 and D_2 are given functions.

Existence, uniqueness and a maximum principle for the solution of this problem is proved in [23]. Numerical experiments and an adaptive algorithm are presented in [24], a priori error estimates are derived in [25].

In this paper, a posteriori error estimates are derived for a semi-discrete finite element approximation of (1)-(4). The error is first bounded above by the equations residual, then by an explicit error estimator. A lower bound is also proposed. Eventhough the tools used to prove that the error is bounded above and below by an error estimator are classical (Clément's interpolant [9] for the upper bound, bubble functions [5] for the lower bound), the model problem is parabolic and nonlinear, which makes the analysis original and not so obvious. Moreover, the regularity requirements to prove the upper bound meet those established in the existence proof [23]. Numerical results are proposed on uniform meshes, showing that the estimates are sharp, the effectivity index being of order one, which may be surprisingly good for such a nonlinear problem. Finally, an adaptive finite element procedure is validated and the computation of a solutal dendrite is presented.

2 Modeling the solidification of a binary alloy

In this section we follow [22,26] and briefly present the modeling corresponding to (1)-(4). A similar model was also presented in [27]. Consider the solidification a binary alloy contained in a smooth domain Ω of $\mathbb{R}^2$, between time 0 and T. The alloy is characterized by its temperature θ, relative concentration c (the proportion of solute in the solvent) and order parameter ϕ, which are scalar functions defined on $\Omega \times (0,T)$. When $\phi = 1$ the alloy is considered to be liquid, $\phi = 0$ the alloy is solid. The region where $0 < \phi < 1$ has small width compared to the size of the calculation domain Ω, and corresponds to the solid-liquid interface (it is sometimes called the mushy region).

The model derivation starts from mass conservation of the solute :

$$\frac{\partial c}{\partial t} + \text{div } \mathbf{j}_c = 0 \qquad \text{in } \Omega \times (0,T). \tag{5}$$

Here $\mathbf{j}_c$ denotes the mass flux of solute and is determined as following. At time t, the free energy of the system is defined by

$$\mathcal{F}(t) = \int_\Omega \left(f(\theta(x,t), c(x,t), \phi(x,t)) + \frac{\tilde{\varepsilon}^2}{2} |\nabla \phi(x,t)|^2 \right) dx, \tag{6}$$

where f is the free energy density of the alloy and $\tilde{\varepsilon}$ is a given parameter. From the second principle of thermodynamics, $\mathcal{F}(t)$ has to decrease. We thus

compute $\mathcal{F}'(t)$ and obtain :

$$\mathcal{F}'(t) = \int_\Omega \left(\frac{\partial f}{\partial \theta}\frac{\partial \theta}{\partial t} + \frac{\partial f}{\partial c}\frac{\partial c}{\partial t} + \frac{\partial f}{\partial \phi}\frac{\partial \phi}{\partial t} + \tilde{\varepsilon}^2 \nabla\phi \cdot \nabla \frac{\partial \phi}{\partial t} \right) dx.$$

Assuming that the temperature is constant, making use of (5), and integrating by parts we then have

$$\begin{aligned}\mathcal{F}'(t) = &\int_\Omega \left(\mathbf{j}_c \cdot \nabla \frac{\partial f}{\partial c} + \frac{\partial \phi}{\partial t}\left(\frac{\partial f}{\partial \phi} - \tilde{\varepsilon}^2 \Delta\phi \right) \right) dx \\ &+ \int_{\partial\Omega} \left(\tilde{\varepsilon}^2 \nabla\phi \cdot \mathbf{n} \frac{\partial \phi}{\partial t} - \mathbf{j}_c \cdot \mathbf{n} \frac{\partial f}{\partial c} \right) ds.\end{aligned}$$

Clearly, if we choose

$$\begin{aligned} &\mathbf{j}_c = -M_c \nabla \frac{\partial f}{\partial c}, \qquad && \frac{\partial \phi}{\partial t} = -M_\phi \left(\frac{\partial f}{\partial \phi} - \tilde{\varepsilon}^2 \Delta\phi \right), \\ &\mathbf{j}_c \cdot \mathbf{n} = 0, && \nabla\phi \cdot \mathbf{n} = 0, \end{aligned}$$

with $M_c(\theta, c, \phi)$ and M_ϕ strictly positive, then $\mathcal{F}'(t)$ is negative and $\mathcal{F}(t)$ is decreasing. Using (5), we then have

$$\begin{aligned} &\frac{\partial \phi}{\partial t} - M_\phi \tilde{\varepsilon}^2 \Delta\phi = -M_\phi \frac{\partial f}{\partial \phi}, \\ &\frac{\partial c}{\partial t} - \text{div } \left(M_c \nabla \frac{\partial f}{\partial c} \right) = 0, \end{aligned}$$

and the model is complete provided $\tilde{\varepsilon}$, M_ϕ, $M_c(\theta, c, \phi)$ and $f(\theta, c, \phi)$ are known. From thermodynamical considerations [22,26,24], the free energy density of the alloy is given by

$$f(\theta, c, \phi) = (1-c) f^A(\theta, \phi) + c f^B(\theta, \phi) + \frac{R\theta}{v_m}\Big((1-c)\ln\,(1-c) + c\,\ln\, c \Big).$$

Here R and v_m are given parameters and f^A, f^B are the solute and solvent free energy densities defined by

$$\begin{aligned} f^X(\theta, \phi) = &(\theta_m^X - \theta)\left(\frac{e^X + L^X p(\phi)}{\theta_m^X} - C^X \right) \\ &+ C^X \theta\, \ln\, \frac{\theta_m^X}{\theta} + W^X \frac{\theta}{\theta_m^X} g(\phi), \qquad X = A, B. \end{aligned}$$

Here θ_m^X, e^X, L^X, C^X, W^X, $X = A, B$, are given parameters and p, g given polynomials. Typical plots for $f^X(\theta, \phi)$ are shown in figure 1. Finally we obtain equations (1)-(4) setting $D_1 > 0$, $\varepsilon^2 = M_\phi \tilde{\varepsilon}^2$ and defining the functions M_c,

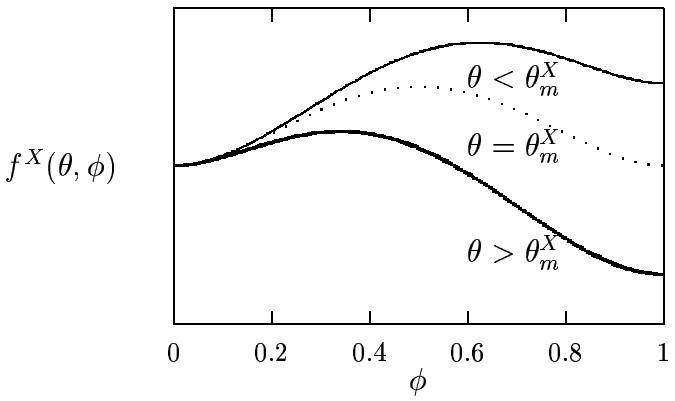

Fig. 1. Free energy density f^X with respect to ϕ, at temperature θ below, equal or above melting temperature θ_m^X.

F_1, F_2, D_2 by

$$
\begin{aligned}
&M_c(\theta,c,\phi) = D_1 \frac{v_m}{R\theta} c(1-c),\\
&F_1(\phi) = M_\phi \left(L^A \frac{\theta-\theta_m^A}{\theta_m^A} p'(\phi) - W^A \frac{\theta}{\theta_m^A} g'(\phi) \right),\\
&F_2(\phi) = M_\phi \left(\left(L^B \frac{\theta-\theta_m^B}{\theta_m^B} - L^A \frac{\theta-\theta_m^A}{\theta_m^A} \right) p'(\phi) - \left(\frac{W^B}{\theta_m^B} - \frac{W^A}{\theta_m^A} \right) \theta g'(\phi) \right),\\
&D_2(c,\phi) = -D_1 \frac{v_m}{R\theta} c(1-c) \frac{F_2(\phi)}{M_\phi}.
\end{aligned}
\tag{7}
$$

Although the original model of [22] makes use of a function $D_1(\phi)$, we have assumed, for the sake of simplicity, D_1 to be constant. However, the theoretical results obtained in [23,25] hold with a Lipschitz, positive, bounded function $D_1(\phi)$. Also, note that formal convergence of this phase-field model towards a Stefan problem with curvature is addressed in [28].

3 Variational formulation and space discretization

We now introduce the weak formulation corresponding to (1)-(4). The notations used are the following. For a given integer $2 \leq p \leq \infty$, we introduce the classical $L^p(\Omega)$, $H^p(\Omega)$ spaces and the corresponding norms $\|\cdot\|_{L^p(\Omega)}$, $\|\cdot\|_{H^p(\Omega)}$, respectively. In order to simplify the notations we set $\|\cdot\|$ instead of $\|\cdot\|_{L^2(\Omega)}$ and $\|\cdot\|_D$ instead of $\|\cdot\|_{L^2(D)}$, where D is a subset of Ω.

Given ϕ_0 and c_0 in $L^2(\Omega)$, the variational formulation corresponding to (1)-(4)

consist in seeking

$$\phi, c \in L^2(0,T;H^1(\Omega)) \cap H^1(0,T;(H^1(\Omega))'),$$

such that $\phi(0) = \phi_0$, $c(0) = c_0$ and

$$\left\langle \frac{\partial \phi}{\partial t}, v \right\rangle + \varepsilon^2 \int_\Omega \nabla\phi \cdot \nabla v = \int_\Omega \Big(F_1(\phi) + cF_2(\phi) \Big) v, \tag{8}$$

$$\left\langle \frac{\partial c}{\partial t}, w \right\rangle + D_1 \int_\Omega \nabla c \cdot \nabla w + \int_\Omega D_2(c,\phi) \nabla\phi \cdot \nabla w = 0, \tag{9}$$

for all $v, w \in H^1(\Omega)$, a.e. in $(0,T)$ (here $< \cdot, \cdot >$ stands for the duality pairing between $H^1(\Omega)$ and its dual). In the sequel, we will assume that

$$\begin{array}{l} F_1,\ F_2 \text{ and } D_2 \text{ are smooth Lipschitz bounded functions} \\ \text{such that } F_i(0) = F_i(1) = 0,\ i = 1,2 \text{ and } D_2(0,\cdot) = D_2(1,\cdot) = 0. \end{array} \tag{10}$$

Then, according to [23] (theorem 1), there is a solution to the above problem. Moreover, we assume that

$$\phi_0 \in H^2(\Omega) \text{ with } \partial\phi_0/\partial n = 0 \text{ on } \partial\Omega \text{ and } c_0 \in H^1(\Omega), \tag{11}$$

so that, according to [23] (theorem 2), the solution is unique,

$$\begin{array}{c} \phi \in L^2([0,T];H^3(\Omega)) \cap H^1([0,T];H^1(\Omega)), \\ c \in L^2([0,T];H^2(\Omega)) \cap H^1([0,T];L^2(\Omega)), \end{array}$$

thus ϕ belongs to $C^0([0,T];H^2(\Omega))$ and c belongs to $C^0([0,T];H^1(\Omega))$. Finally, we assume that

$$\begin{array}{l} F_1 \text{ and } F_2 \text{ are zero outside the interval (0,1)} \\ \text{and that } \phi_0,\ c_0 \text{ are between 0 and 1,} \end{array} \tag{12}$$

so that, according to [23] (theorem 3), a maximum principle holds and ϕ, c are also between 0 and 1. Thus, the solution to problem (1)-(4) has a physical meaning and all the nonlinear terms in (7) can be truncated to zero outside the interval $[0,1]$. This allows assumptions (10) and (12) to be fulfilled, and the existence result to hold. Finally, this being useless in our proofs, we mention that the space regularity of c is one order lower than the space regularity of ϕ, due to the div $(D_2(c,\phi)\nabla\phi)$ term in eq. (2).

Let us now turn to the semi-discrete finite element approximation of (8) (9). From now on, it is assumed that the calculation domain Ω is polygonal and that the existence and regularity results presented above still hold. For any $0 < h < 1$, $\mathcal{T}_h$ be a mesh of $\overline{\Omega}$ into triangles K with diameter less than h, regular in the sense of [29]. Let $V_h = \{v \in \mathcal{C}^0(\overline{\Omega})\ ;\ v_{|K} \in \mathbb{P}_1\ ;\ \forall K \in \mathcal{T}_h\}$

be the usual finite element space of continuous, piecewise linear functions on the triangles of $\mathcal{T}_h$ and let $r_h : \mathcal{C}^0(\overline{\Omega}) \to V_h$ be the corresponding Lagrange interpolant. The semi-discrete finite element problem corresponding to (8) (9) is the following. Assuming ϕ_0 and c_0 to be continuous, we set $\phi_h(0) = r_h\phi_0$ $c_h(0) = r_h c_0$. For each $t \in [0,T]$ find $\phi_h(t)$ and $c_h(t)$ in V_h such that

$$\int_\Omega \frac{\partial \phi_h}{\partial t} v_h + \varepsilon^2 \int_\Omega \nabla\phi_h \cdot \nabla v_h = \int_\Omega \Big(F_1(\phi_h) + c_h F_2(\phi_h) \Big) v_h, \tag{13}$$

$$\int_\Omega \frac{\partial c_h}{\partial t} w_h + D_1 \int_\Omega \nabla c_h \cdot \nabla w_h + \int_\Omega D_2(c_h, \phi_h) \nabla\phi_h \cdot \nabla w_h = 0, \tag{14}$$

for all $v_h, w_h \in V_h$. In the sequel, we will assume that the above semi-discretized problem is well posed (this could be proved proceeding as in [23]) and that a priori error estimates are available for the error

$$\int_0^T \Big(\|\nabla(\phi - \phi_h)\|^2 + \|\nabla(c - c_h)\|^2 \Big).$$

In order to derive sharp a posteriori error estimates, we also need to assume that the error in the $L^2(0,T;L^2(\Omega))$ norm converges faster than the error in the $L^2(0,T;H^1(\Omega))$ norm, that is there are two constant $C > 0$ and $s \in]0,1]$ independent of h such that

$$\int_0^T \Big(\|\phi - \phi_h\|^2 + \|c - c_h\|^2 \Big) \leq C h^{2s} \int_0^T \Big(\|\nabla(\phi - \phi_h)\|^2 + \|\nabla(c - c_h)\|^2 \Big). \tag{15}$$

Remark 1 *Let us discuss assumption (15). Assume for instance that optimal a priori error estimates are available, i.e. the error in the $L^2(0,T;L^2(\Omega))$ norm is properly $O(h^2)$ and the error in the $L^2(0,T;H^1(\Omega))$ norm is properly $O(h)$. Then (15) holds with $s = 1$.*

Proving a priori error estimates for our model problem is not an obvious task. In [25], it is proved that the error in the $L^\infty(0,T;L^2(\Omega))$ norm is bounded by a constant time $(h^2 + \tau)$ for the corresponding problem discretized in space and time, τ being the time step. A similar a priori estimate could be proved for problem (13) (14), but this is out of the scope of this paper. Moreover, to prove assumption (15), one should also prove that the error in the $L^2(0,T;H^1(\Omega))$ norm is greater than a constant times h (or eventually h^s with $s \in (0,1]$), which is generally an assumption, even for the Laplace problem, see [6] theorem 3.2 (in fact, for the Laplace problem, assumption (15) is valid except for trivial cases, see [30]). Finally, note that an assumption similar to (15) was previously used in [31] in the frame of a stationary nonlinear convection-diffusion problem.

4 An upper bound

The first step in deriving a posteriori error estimates consists in bounding the error by the equations residual $R_\phi(\phi_h, c_h)$ and $R_c(\phi_h, c_h)$ defined by

$$R_\phi(\phi_h, c_h), R_c(\phi_h, c_h) \in (H^1(\Omega))' \text{ a.e. in } (0,T)$$

and

$$< R_\phi(\phi_h, c_h), v >= \int_\Omega \left(\frac{\partial \phi_h}{\partial t} v + \varepsilon^2 \nabla \phi_h \cdot \nabla v - F_1(\phi_h) v - c_h F_2(\phi_h) v \right), \quad (16)$$

$$< R_c(\phi_h, c_h), v >= \int_\Omega \left(\frac{\partial c_h}{\partial t} v + D_1 \nabla c_h \cdot \nabla v + D_2(c_h, \phi_h) \nabla \phi_h \cdot \nabla v \right), \quad (17)$$

for all $v \in H^1(\Omega)$, a.e. in $(0,T)$. More precisely, we have the following result.

Proposition 2 *Assume that (10), (11), (12) and (15) hold. Let ϕ, c be the solution of (8) (9), let ϕ_h, c_h be the solution of (13) (14) and let $R_\phi(\phi_h, c_h)$, $R_c(\phi_h, c_h)$ be defined by (16) (17). Finally, let M_2 be defined by $M_2 = \|D_2\|_{L^\infty(\mathbb{R}^2)}$. Then, there exists $h_0 > 0$ (depending only on the constant C of (15), on ε, D_1 and M_2) such that, for all $h \le h_0$, we have*

$$\begin{aligned}
&\frac{1}{2}\|(\phi - \phi_h)(T)\|^2 + \frac{\varepsilon^2}{2}\int_0^T \|\nabla(\phi - \phi_h)\|^2 \\
&+ \frac{\varepsilon^2 D_1}{8M_2^2}\|(c - c_h)(T)\|^2 + \frac{\varepsilon^2 D_1^2}{8M_2^2}\int_0^T \|\nabla(c - c_h)\|^2 \\
&\le \frac{1}{2}\|(\phi - \phi_h)(0)\|^2 + \frac{\varepsilon^2 D_1}{8M_2^2}\|(c - c_h)(0)\|^2 \\
&+ \left| \int_0^T < R_\phi(\phi_h, c_h), \phi - \phi_h > \right| + \frac{\varepsilon^2 D_1}{4M_2^2} \left| \int_0^T < R_c(\phi_h, c_h), c - c_h > \right|.
\end{aligned} \quad (18)$$

PROOF. Using (8) we have

$$\begin{aligned}
&\left\langle \frac{\partial}{\partial t}(\phi - \phi_h), \phi - \phi_h \right\rangle + \int_\Omega \varepsilon^2 |\nabla(\phi - \phi_h)|^2 \\
&= \int_\Omega \left(F_1(\phi) + cF_2(\phi) - \frac{\partial \phi_h}{\partial t} \right)(\phi - \phi_h) \\
&- \int_\Omega \varepsilon^2 \nabla \phi_h \cdot \nabla(\phi - \phi_h).
\end{aligned}$$

Integrating between $t = 0$ and $t = T$ and using the definition (16) we obtain

$$\begin{aligned}
&\frac{1}{2}\|(\phi-\phi_h)(T)\|^2 + \varepsilon^2 \int_0^T \|\nabla(\phi-\phi_h)\|^2 \\
&\leq \frac{1}{2}\|(\phi-\phi_h)(0)\|^2 + \left| \int_0^T < R_\phi(\phi_h, c_h), \phi-\phi_h > \right| \\
&+ \left| \int_0^T \int_\Omega \Big(F_1(\phi) - F_1(\phi_h) + cF_2(\phi) - c_h F_2(\phi_h) \Big)(\phi-\phi_h) \right|.
\end{aligned} \tag{19}$$

On the other hand, using (9) we have

$$\begin{aligned}
&\left\langle \frac{\partial}{\partial t}(c-c_h), (c-c_h) \right\rangle + \int_\Omega D_1 |\nabla(c-c_h)|^2 \\
&= \int_\Omega \left(-D_2(c,\phi)\nabla\phi\cdot\nabla(c-c_h) - \frac{\partial c_h}{\partial t}(c-c_h) \right) \\
&- D_1 \int_\Omega \nabla c_h \cdot \nabla(c-c_h).
\end{aligned}$$

Thus, a time integration between $t = 0$ and $t = T$ and the use of definition (17) leads to

$$\begin{aligned}
&\frac{1}{2}\|(c-c_h)(T)\|^2 + D_1 \int_0^T \|\nabla(c-c_h)\|^2 \\
&\leq \frac{1}{2}\|(c-c_h)(0)\|^2 + \left| \int_0^T < R_c(\phi_h, c_h), c-c_h > \right| \\
&+ \left| \int_0^T \int_\Omega \Big(D_2(c_h,\phi_h)\nabla\phi_h - D_2(c,\phi)\nabla\phi \Big) \cdot \nabla(c-c_h) \right|.
\end{aligned} \tag{20}$$

Let α be a real positive number that will be chosen in the sequel. Adding (19) and α times (20) yields

$$\begin{aligned}
&\frac{1}{2}\|(\phi-\phi_h)(T)\|^2 + \varepsilon^2 \int_0^T \|\nabla(\phi-\phi_h)\|^2 \\
&\frac{\alpha}{2}\|(c-c_h)(T)\|^2 + \alpha D_1 \int_0^T \|\nabla(c-c_h)\|^2 \\
&\leq \frac{1}{2}\|(\phi-\phi_h)(0)\|^2 + \frac{\alpha}{2}\|(c-c_h)(0)\|^2 \\
&+ \left| \int_0^T < R_\phi(\phi_h, c_h), \phi-\phi_h > \right| + \alpha \left| \int_0^T < R_c(\phi_h, c_h), c-c_h > \right| \\
&+ \left| \int_0^T \int_\Omega \Big(F_1(\phi) - F_1(\phi_h) + cF_2(\phi) - c_h F_2(\phi_h) \Big)(\phi-\phi_h) \right| \\
&+ \alpha \left| \int_0^T \int_\Omega \Big(D_2(c_h,\phi_h)\nabla\phi_h - D_2(c,\phi)\nabla\phi \Big) \cdot \nabla(c-c_h) \right|.
\end{aligned} \tag{21}$$

We now focus on the last two terms of (21). Since F_1 is Lipschitz there is a constant C independent of h such that

$$\left|\int_0^T \int_\Omega \Big(F_1(\phi) - F_1(\phi_h)\Big)(\phi - \phi_h)\right| \leq C \int_0^T \|\phi - \phi_h\|^2.$$

Since F_2 is Lipschitz bounded and c is bounded above by 1, we have

$$\begin{aligned}
&\left|\int_0^T \int_\Omega \Big(cF_2(\phi) - c_h F_2(\phi_h)\Big)(\phi - \phi_h)\right| \\
&\quad = \left|\int_0^T \int_\Omega \Big(c\Big(F_2(\phi) - F_2(\phi_h)\Big) + F_2(\phi_h)(c - c_h)\Big)(\phi - \phi_h)\right| \\
&\quad \leq C \int_0^T \|\phi - \phi_h\|\Big(\|\phi - \phi_h\| + \|c - c_h\|\Big).
\end{aligned}$$

Using the two above estimates together with (15), there is a constant C independent of h such that

$$\begin{aligned}
&\left|\int_0^T \int_\Omega \Big(F_1(\phi) - F_1(\phi_h) + cF_2(\phi) - c_h F_2(\phi_h)\Big)(\phi - \phi_h)\right| \\
&\qquad \leq Ch^{2s} \int_0^T \Big(\|\nabla(\phi - \phi_h)\|^2 + \|\nabla(c - c_h)\|^2\Big).
\end{aligned} \tag{22}$$

Let us now turn to the last term of (21). We have

$$\begin{aligned}
&\Big(D_2(c_h, \phi_h)\nabla\phi_h - D_2(c, \phi)\nabla\phi\Big) \cdot \nabla(c - c_h) \\
&\qquad = -\Big(D_2(c, \phi) - D_2(c_h, \phi_h)\Big)\nabla\phi \cdot \nabla(c - c_h) \\
&\qquad - D_2(c_h, \phi_h)\nabla(\phi - \phi_h) \cdot \nabla(c - c_h).
\end{aligned}$$

Since D_2 is bounded by M_2, using Young's inequality, we obtain

$$\begin{aligned}
&\left|\int_0^T \int_\Omega D_2(c_h, \phi_h)\nabla(\phi - \phi_h) \cdot \nabla(c - c_h)\right| \\
&\qquad \leq M_2 \int_0^T \Big(\frac{1}{2\eta}\|\nabla(\phi - \phi_h)\|^2 + \frac{\eta}{2}\|\nabla(c - c_h)\|^2\Big),
\end{aligned} \tag{23}$$

where $\eta > 0$ will be chosen in the sequel. On the other hand, using Hölder inequality, we obtain

$$\begin{aligned}
&\left|\int_0^T \int_\Omega \Big(D_2(c, \phi) - D_2(c_h, \phi_h)\Big)\nabla\phi \cdot \nabla(c - c_h)\right| \\
&\qquad \leq \int_0^T \|\nabla\phi\|_{L^6(\Omega)} \|D_2(c, \phi) - D_2(c_h, \phi_h)\|_{L^3(\Omega)} \|\nabla(c - c_h)\|.
\end{aligned} \tag{24}$$

Since the imbedding between $H^1(\Omega)$ and $L^6(\Omega)$ is continuous and since $\phi \in C^0([0, T]; H^2(\Omega))$, then $\|\nabla\phi\|_{L^6(\Omega)}$ is bounded for each $t \in [0, T]$. Moreover,

since D_2 is Lipschitz we have

$$\|D_2(c,\phi) - D_2(c_h,\phi_h)\|_{L^3(\Omega)} \leq C\Big(\|\phi-\phi_h\|_{L^3(\Omega)} + \|c-c_h\|_{L^3(\Omega)}\Big).$$

The above estimate in (24) yields

$$\begin{aligned}
&\left|\int_0^T \int_\Omega \Big(D_2(c,\phi) - D_2(c_h,\phi_h)\Big)\nabla\phi\cdot\nabla(c-c_h)\right| \\
&\qquad \leq C\int_0^T \Big(\|\phi-\phi_h\|_{L^3(\Omega)} + \|c-c_h\|_{L^3(\Omega)}\Big)\|\nabla(c-c_h)\|.
\end{aligned}$$

We now use a Gagliardo-Nirenberg inequality [32] to obtain

$$\begin{aligned}
&\left|\int_0^T \int_\Omega \Big(D_2(c,\phi) - D_2(c_h,\phi_h)\Big)\nabla\phi\cdot\nabla(c-c_h)\right| \\
&\qquad \leq C\int_0^T \Big(\|\phi-\phi_h\|^{1/2}_{H^1(\Omega)}\|\phi-\phi_h\|^{1/2} \\
&\qquad\qquad + \|c-c_h\|^{1/2}_{H^1(\Omega)}\|c-c_h\|^{1/2}\Big)\|\nabla(c-c_h)\|.
\end{aligned}$$

Finally, using Cauchy-Schwarz inequality together with (15) we obtain

$$\begin{aligned}
&\left|\int_0^T \int_\Omega \Big(D_2(c,\phi) - D_2(c_h,\phi_h)\Big)\nabla\phi\cdot\nabla(c-c_h)\right| \\
&\qquad \leq Ch^{s/2}\int_0^T \Big(\|\nabla(\phi-\phi_h)\|^2 + \|\nabla(c-c_h)\|^2\Big).
\end{aligned} \tag{25}$$

Estimates (22)-(25) in (21) yield

$$\begin{aligned}
&\frac{1}{2}\|(\phi-\phi_h)(T)\|^2 + \varepsilon^2\int_0^T \|\nabla(\phi-\phi_h)\|^2 \\
&\frac{\alpha}{2}\|(c-c_h)(T)\|^2 + \alpha D_1\int_0^T \|\nabla(c-c_h)\|^2 \\
&\leq \frac{1}{2}\|(\phi-\phi_h)(0)\|^2 + \frac{\alpha}{2}\|(c-c_h)(0)\|^2 \\
&+ \left|\int_0^T < R_\phi(\phi_h,c_h), \phi-\phi_h >\right| + \alpha\left|\int_0^T < R_c(\phi_h,c_h), c-c_h >\right| \\
&+ \alpha M_2\int_0^T \Big(\frac{1}{2\eta}\|\nabla(\phi-\phi_h)\|^2 + \frac{\eta}{2}\|\nabla(c-c_h)\|^2\Big) \\
&+ Ch^{s/2}\int_0^T \Big(\|\nabla(\phi-\phi_h)\|^2 + \|\nabla(c-c_h)\|^2\Big).
\end{aligned} \tag{26}$$

where $\alpha > 0$ and $\eta > 0$. Now let α and η be such that

$$\varepsilon^2 - \frac{\alpha M_2}{2\eta} > 0 \quad \text{and} \quad \alpha D_1 - \frac{\alpha M_2\eta}{2} > 0,$$

for instance we can choose α and η such that

$$\frac{\varepsilon^2}{4} = \frac{\alpha M_2}{2\eta} \quad \text{and} \quad \frac{\alpha D_1}{4} = \frac{\alpha M_2 \eta}{2},$$

that is

$$\eta = \frac{D_1}{2M_2} \quad \text{and} \quad \alpha = \frac{\varepsilon^2 D_1}{4M_2^2}.$$

With this choice (26) becomes

$$\begin{aligned}
&\frac{1}{2}\|(\phi-\phi_h)(T)\|^2 + \frac{3\varepsilon^2}{4}\int_0^T \|\nabla(\phi-\phi_h)\|^2 \\
&\frac{\varepsilon^2 D_1}{8M_2^2}\|(c-c_h)(T)\|^2 + \frac{3\varepsilon^2 D_1^2}{16M_2^2}\int_0^T \|\nabla(c-c_h)\|^2 \\
&\leq \frac{1}{2}\|(\phi-\phi_h)(0)\|^2 + \frac{\varepsilon^2 D_1}{8M_2^2}\|(c-c_h)(0)\|^2 \\
&+ \left|\int_0^T < R_\phi(\phi_h, c_h), \phi-\phi_h > \right| + \frac{\varepsilon^2 D_1}{4M_2^2}\left|\int_0^T < R_c(\phi_h, c_h), c-c_h > \right| \\
&+ Ch^{s/2}\int_0^T \Big(\|\nabla(\phi-\phi_h)\|^2 + \|\nabla(c-c_h)\|^2\Big).
\end{aligned} \tag{27}$$

Let h_0 be such that

$$Ch_0^{s/2} < \frac{3\varepsilon^2}{4} \quad \text{and} \quad Ch_0^{s/2} < \frac{3\varepsilon^2 D_1}{16M_2^2}.$$

For instance we can choose h_0 such that

$$Ch_0^{s/2} = \min\left(\frac{\varepsilon^2}{4}, \frac{\varepsilon^2 D_1^2}{16M_2^2}\right),$$

and we obtain (18) for $h \leq h_0$. □

Our goal is now to provide an upper bound for the equations residual $R_\phi(\phi_h, c_h)$ and $R_c(\phi_h, c_h)$ defined in (16) (17). For this purpose, an explicit error estimator is introduced.

The notations are those of [6]. For any triangle K of the triangulation $\mathcal{T}_h$, let E_K be the set of its three edges. For each interior edge ℓ of $\mathcal{T}_h$, let us choose an arbitrary normal direction $\mathbf{n}$, let $[\nabla\phi_h \cdot \mathbf{n}]_\ell$ denote the jump of $\nabla\phi_h \cdot \mathbf{n}$ across the edge ℓ. For each edge ℓ of $\mathcal{T}_h$ lying on the boundary $\partial\Omega$, we set $[\nabla\phi_h \cdot \mathbf{n}]_\ell = 2\nabla\phi_h \cdot \mathbf{n}$. The local error estimator corresponding to equation (1)

is then defined by

$$\eta_K^2 = h_K^2 \left\| \frac{\partial \phi_h}{\partial t} - \varepsilon^2 \Delta \phi_h - F_1(\phi_h) - c_h F_2(\phi_h) \right\|_K^2 + \frac{1}{2} \sum_{\ell \in E_K} |\ell| \left\| \varepsilon^2 \left[\nabla \phi_h \cdot \mathbf{n} \right] \right\|_\ell^2 \tag{28}$$

for all $K \in \mathcal{T}_h$. Similarly, the local error estimator corresponding to equation (2) is defined by

$$\mu_K^2 = h_K^2 \left\| \frac{\partial c_h}{\partial t} - D_1 \Delta c_h - \text{div } \left(D_2(c_h, \phi_h) \nabla \phi_h \right) \right\|_K^2 + \frac{1}{2} \sum_{\ell \in E_K} |\ell| \left\| \left[\left(D_1 \nabla c_h + D_2(c_h, \phi_h) \nabla \phi_h \right) \cdot \mathbf{n} \right] \right\|_\ell^2 . \tag{29}$$

Using the same techniques as in [9,19], we can prove the following result.

Proposition 3 *Let ϕ_h, c_h be the solution of (13) (14), let $R_\phi(\phi_h, c_h)$, $R_c(\phi_h, c_h)$ be defined by (16) (17) and let η_K^2, μ_K^2 be defined by (28) (29). Then, there is a constant C depending only on the shape of the triangles of the mesh $\mathcal{T}_h$ such that, for all $v \in L^2(0,T;H^1(\Omega))$ we have*

$$\begin{aligned} \left| \int_0^T < R_\phi(\phi_h, c_h), v > \right| &\leq C \left(\int_0^T \sum_{K \in \mathcal{T}_h} \eta_K^2 \right)^{1/2} \\ &\quad \left(\int_0^T \left(\|v\|^2 + \|\nabla v\|^2 \right) \right)^{1/2} , \\ \left| \int_0^T < R_c(\phi_h, c_h), v > \right| &\leq C \left(\int_0^T \sum_{K \in \mathcal{T}_h} \mu_K^2 \right)^{1/2} \\ &\quad \left(\int_0^T \left(\|v\|^2 + \|\nabla v\|^2 \right) \right)^{1/2} . \end{aligned} \tag{30}$$

PROOF. We will only sketch the proof for the first estimate. The second estimate can be obtained in the same manner. Let v be an element of $L^2(0,T;H^1(\Omega))$. Using (13) and (16) we have

$$< R_\phi(\phi_h, c_h), v > = < R_\phi(\phi_h, c_h), v - v_h > \qquad \forall v_h \in V_h \quad \text{a.e. in } (0,T).$$

From the definition of $R_\phi(\phi_h, c_h)$ we have

$$< R_\phi(\phi_h, c_h), v - v_h >= \sum_{K\in\mathcal{T}_h} \Bigg\{ \int_K \left(\frac{\partial \phi_h}{\partial t} - F_1(\phi_h) - c_h F_2(\phi_h) \right) (v - v_h) + \int_K \varepsilon^2 \nabla \phi_h \cdot \nabla (v - v_h) \Bigg\}.$$

Integrating by parts the last term we obtain

$$\begin{aligned} &< R_\phi(\phi_h, c_h), v - v_h > \\ &\quad = \sum_{K\in\mathcal{T}_h} \Bigg\{ \int_K \left(\frac{\partial \phi_h}{\partial t} - \varepsilon^2 \Delta \phi_h - F_1(\phi_h) - c_h F_2(\phi_h) \right) (v - v_h) \\ &\qquad + \frac{1}{2} \sum_{\ell\in E_K} \varepsilon^2 \int_\ell [\nabla \phi_h \cdot \mathbf{n}] (v - v_h) \Bigg\}. \end{aligned}$$

Thus, Cauchy-Schwarz inequality yields

$$\begin{aligned} &| < R_\phi(\phi_h, c_h), v - v_h > | \\ &\quad \le \sum_{K\in\mathcal{T}_h} \Bigg\{ \left\| \frac{\partial \phi_h}{\partial t} - \varepsilon^2 \Delta \phi_h - F_1(\phi_h) - c_h F_2(\phi_h) \right\|_K \|v - v_h\|_K \\ &\qquad + \frac{1}{2} \sum_{\ell\in E_K} \varepsilon^2 \left\| [\nabla \phi_h \cdot \mathbf{n}] \right\|_\ell \|v - v_h\|_\ell \Bigg\}. \end{aligned} \tag{31}$$

We then choose, a.e. in $(0, T)$, $v_h = R_h v$ Clément's interpolant [33,9], thus there is a constant C depending only on the shape of the mesh elements such that

$$\begin{aligned} \|v - R_h v\|_K^2 &\le C h_K^2 \Big(\|v\|_{\Delta K}^2 + \|\nabla v\|_{\Delta K}^2 \Big), \\ \|v - R_h v\|_\ell^2 &\le C |\ell| \Big(\|v\|_{\Delta K}^2 + \|\nabla v\|_{\Delta K}^2 \Big), \end{aligned} \tag{32}$$

where ΔK denotes the set of triangles having a common edge or vertex with K. Using (32) in (31) yields

$$\begin{aligned} &| < R_\phi(\phi_h, c_h), v - v_h > | \\ &\qquad \le C \left(\sum_{K\in\mathcal{T}_h} \eta_K^2 \right)^{1/2} \left(\sum_{K\in\mathcal{T}_h} \Big(\|v\|_{\Delta K}^2 + \|\nabla v\|_{\Delta K}^2 \Big) \right)^{1/2}. \end{aligned} \tag{33}$$

Since the mesh is regular, there is a constant C depending only on the shape of the mesh elements such that

$$\sum_{K\in\mathcal{T}_h} \Big(\|v\|_{\Delta K}^2 + \|\nabla v\|_{\Delta K}^2 \Big) \le C \Big(\|v\|^2 + \|\nabla v\|^2 \Big)$$

Integrating (33) between 0 and T thus yields

$$\left| \int_0^T < R_\phi(\phi_h, c_h), v - v_h > \right| \leq C \int_0^T \left(\sum_{K \in \mathcal{T}_h} \eta_K^2 \right)^{1/2} \left(\|v\|^2 + \|\nabla v\|^2 \right)^{1/2},$$

and finally, Cauchy-Schwarz inequality yields the result. □

Putting together the results of propositions 2 and 3 we can bound the error by the estimator. For this purpose we need one more assumption in order to control the initial error. We will assume that the initial error converges faster than the error in the $L^2(0,T;H^1(\Omega))$ norm. Thus, there are two constant $C > 0$ and $r \in]0,1]$ independent of h such that

$$\|(\phi - \phi_h)(0)\|^2 + \|(c - c_h)(0)\|^2 \leq C h^{2r} \int_0^T \left(\|\nabla(\phi - \phi_h)\|^2 + \|\nabla(c - c_h)\|^2 \right). \quad (34)$$

Remark 4 *As in remark 1, let us discuss assumption (34). Assume for instance that optimal error estimates are available. For instance if ϕ_0 and c_0 are in $H^2(\Omega)$ and since we choosed $\phi_h(0) = r_h\phi_0$, $c_h(0) = r_h c_0$, then the initial error in the $L^2(\Omega)$ norm is $O(h^2)$ whereas the error in the $L^2(0,T;H^1(\Omega))$ norm is properly $O(h)$. Then (34) holds with $r = 1$.*

Theorem 5 *Assume that (10), (11), (12), (15) and (34) hold. Let ϕ, c be the solution of (8) (9), let ϕ_h, c_h be the solution of (13) (14) and let η_K^2, μ_K^2 be defined by (28) (29). Finally, let M_2 be defined by $M_2 = \|D_2\|_{L^\infty(\mathbb{R}^2)}$. Then, there is a constant C depending only on the shape of the mesh elements such that, for h sufficiently small, we have*

$$\begin{aligned} &\varepsilon^2 \int_0^T \|\nabla(\phi - \phi_h)\|^2 + \frac{\varepsilon^2 D_1^2}{4M_2^2} \int_0^T \|\nabla(c - c_h)\|^2 \\ &\leq C \left(\frac{1}{\varepsilon^2} \int_0^T \sum_{K \in \mathcal{T}_h} \eta_K^2 + \frac{\varepsilon^2}{2M_2^2} \int_0^T \sum_{K \in \mathcal{T}_h} \mu_K^2 \right). \end{aligned} \quad (35)$$

PROOF. Putting (30) in (18) yields

$$\begin{aligned}
&\frac{\varepsilon^2}{2}\int_0^T \|\nabla(\phi-\phi_h)\|^2 + \frac{\varepsilon^2 D_1^2}{8M_2^2}\int_0^T \|\nabla(c-c_h)\|^2 \\
&\leq \frac{1}{2}\|(\phi-\phi_h)(0)\|^2 + \frac{\varepsilon^2 D_1}{8M_2^2}\|(c-c_h)(0)\|^2 \\
&+ C\Bigg\{\left(\int_0^T \sum_{K\in\mathcal{T}_h}\eta_K^2\right)^{1/2}\left(\int_0^T\left(\|\phi-\phi_h\|^2+\|\nabla(\phi-\phi_h)\|^2\right)\right)^{1/2} \\
&+ \frac{\varepsilon^2 D_1}{4M_2^2}\left(\int_0^T \sum_{K\in\mathcal{T}_h}\mu_K^2\right)^{1/2}\left(\int_0^T\left(\|c-c_h\|^2+\|\nabla(c-c_h)\|^2\right)\right)^{1/2}\Bigg\},
\end{aligned} \tag{36}$$

where C depends only on the shape of the mesh triangles. Using (15) and (34) yields, for h small enough :

$$\begin{aligned}
&\varepsilon^2\int_0^T \|\nabla(\phi-\phi_h)\|^2 + \frac{\varepsilon^2 D_1^2}{4M_2^2}\int_0^T \|\nabla(c-c_h)\|^2 \\
&\leq C\Bigg\{\left(\int_0^T \sum_{K\in\mathcal{T}_h}\eta_K^2\right)^{1/2}\left(\int_0^T\|\nabla(\phi-\phi_h)\|^2\right)^{1/2} \\
&+ \frac{\varepsilon^2 D_1}{4M_2^2}\left(\int_0^T \sum_{K\in\mathcal{T}_h}\mu_K^2\right)^{1/2}\left(\int_0^T\|\nabla(c-c_h)\|^2\right)^{1/2}\Bigg\}.
\end{aligned} \tag{37}$$

We conclude by using Young's inequality.

5 A Lower bound

In order to prove that the error estimator is bounded above by the true error, we proceed as in [6,5,19] and introduce the error estimators $\tilde{\eta}_K$ and $\tilde{\mu}_K$ defined by

$$\begin{aligned}
\tilde{\eta}_K^2 &= |K|^2\left(\Pi_K\left(\frac{\partial\phi_h}{\partial t} - \varepsilon^2\Delta\phi_h - F_1(\phi_h) - c_h F_2(\phi_h)\right)\right)^2 \\
&+ \frac{1}{2}\sum_{\ell\in E_K}|\ell|^2\left(\varepsilon^2\left[\nabla\phi_h\cdot\mathbf{n}\right]\right)^2, \\
\tilde{\mu}_K^2 &= |K|^2\left(\Pi_K\left(\frac{\partial c_h}{\partial t} - D_1\Delta c_h - \text{div }\left(D_2(c_h,\phi_h)\nabla\phi_h\right)\right)\right)^2 \\
&+ \frac{1}{2}\sum_{\ell\in E_K}|\ell|^2\left[\left(D_1\nabla c_h + \Pi_\ell(D_2(c_h,\phi_h)\nabla\phi_h)\right)\cdot\mathbf{n}\right]^2.
\end{aligned} \tag{38}$$

Here Π_K (resp. Π_ℓ) is the $L^2(K)$-projection (resp. $L^2(\ell)$-projection) onto the constants. In the following lemma, we prove that the error estimators η_K and

μ_K are bounded by $\tilde{\eta}_K$ and $\tilde{\mu}_K$, respectively.

Lemma 6 *There is a constant C depending only on the shape of the mesh triangles, such that, for all $K \in \mathcal{T}_h$, we have*

$$\begin{aligned}
\eta_K^2 \leq C\Bigg(\tilde{\eta}_K^2 + h_K^3 \Bigg\| \nabla\left(\frac{\partial \phi_h}{\partial t} - \varepsilon^2 \Delta \phi_h - F_1(\phi_h) - c_h F_2(\phi_h)\right)\Bigg\|_K \\
\Bigg\|\frac{\partial \phi_h}{\partial t} - \varepsilon^2 \Delta \phi_h - F_1(\phi_h) - c_h F_2(\phi_h)\Bigg\|_K\Bigg) \\
\mu_K^2 \leq C\Bigg(\tilde{\mu}_K^2 + h_K^3 \Bigg\| \nabla\left(\frac{\partial c_h}{\partial t} - D_1 \Delta c_h - div\ (D_2(c_h,\phi_h)\nabla\phi_h)\right)\Bigg\|_K \\
\Bigg\|\frac{\partial c_h}{\partial t} - D_1 \Delta c_h - div\ (D_2(c_h,\phi_h)\nabla\phi_h)\Bigg\|_K \\
+ \sum_{\ell \in E_K} |\ell|^2 \left\|[\nabla(D_2(c_h,\phi_h)\nabla\phi_h \cdot \mathbf{n})]\right\|_\ell \\
\left\|[D_2(c_h,\phi_h)\nabla\phi_h \cdot \mathbf{n}]\right\|_\ell\Bigg).
\end{aligned} \tag{39}$$

PROOF. Let us start with the first estimate of (39). Since the mesh is regular, there is a constant C depending only on the shape of the mesh elements such that $h_K^2 \leq C|K|$ and therefore

$$\eta_K^2 \leq C\Big(\tilde{\eta}_K^2 + |K|\delta_K(\phi_h, c_h)\Big), \tag{40}$$

where we have set

$$\begin{aligned}
\delta_K(\phi_h, c_h) = \int_K \left(\frac{\partial \phi_h}{\partial t} - \varepsilon^2 \Delta \phi_h - F_1(\phi_h) - c_h F_2(\phi_h)\right)^2 \\
- \int_K \left(\Pi_K\left(\frac{\partial \phi_h}{\partial t} - \varepsilon^2 \Delta \phi_h - F_1(\phi_h) - c_h F_2(\phi_h)\right)\right)^2.
\end{aligned}$$

From standard interpolation results on Π_K, there is a constant C depending only on the shape of the mesh elements such that, for any $f \in H^1(K)$ we have

$$\int_K f^2 - (\Pi_K f)^2 = \int_K (f - \Pi_K f) f \leq C h_K \|\nabla f\|_K \|f\|_K,$$

so that

$$\begin{aligned}
\delta_K(\phi_h, c_h) \leq C h_K \Bigg\| \nabla\left(\frac{\partial \phi_h}{\partial t} - \varepsilon^2 \Delta \phi_h - F_1(\phi_h) - c_h F_2(\phi_h)\right)\Bigg\|_K \\
\Bigg\|\frac{\partial \phi_h}{\partial t} - \varepsilon^2 \Delta \phi_h - F_1(\phi_h) - c_h F_2(\phi_h)\Bigg\|_K.
\end{aligned}$$

The above estimate in (40) proves the first estimate of (39).

We proceed in the same manner to prove the second estimate of (39). We have

$$\mu_K^2 \leq C \left(\tilde{\mu}_K^2 + |K| \delta_K(\phi_h, c_h) + \frac{1}{2} \sum_{\ell \in E_K} |\ell| \delta_\ell(\phi_h, c_h) \right), \tag{41}$$

where $\delta_K(\phi_h, c_h)$ is now defined by

$$\begin{aligned} \delta_K(\phi_h, c_h) = & \int_K \left(\frac{\partial c_h}{\partial t} - D_1 \Delta c_h - \text{div } (D_2(c_h, \phi_h) \nabla \phi_h) \right)^2 \\ & - \int_K \left(\Pi_K \left(\frac{\partial c_h}{\partial t} - D_1 \Delta c_h - \text{div } (D_2(c_h, \phi_h) \nabla \phi_h) \right) \right)^2, \end{aligned}$$

and $\delta_\ell(\phi_h, c_h)$ by

$$\begin{aligned} \delta_\ell(\phi_h, c_h) = & \int_\ell \Big[D_2(c_h, \phi_h) \nabla \phi_h \cdot \mathbf{n} \Big]^2 \\ & - \int_\ell \Big[\Pi_\ell (D_2(c_h, \phi_h) \nabla \phi_h \cdot \mathbf{n}) \Big]^2. \end{aligned}$$

From the interpolation properties of Π_K, there is a constant C depending only on the shape of the mesh elements such that

$$\begin{aligned} \delta_K(\phi_h, c_h) \leq C h_K & \left\| \nabla \left(\frac{\partial c_h}{\partial t} - D_1 \Delta c_h - \text{div } (D_2(c_h, \phi_h) \nabla \phi_h) \right) \right\|_K \\ & \left\| \frac{\partial c_h}{\partial t} - D_1 \Delta c_h - \text{div } (D_2(c_h, \phi_h) \nabla \phi_h) \right\|_K. \end{aligned} \tag{42}$$

From the interpolation properties of Π_ℓ, there is a constant C depending only on the shape of the mesh elements such that

$$\delta_\ell(\phi_h, c_h) \leq C |\ell| \, \| [\nabla (D_2(c_h, \phi_h) \nabla \phi_h \cdot \mathbf{n})] \|_\ell \, \| [D_2(c_h, \phi_h) \nabla \phi_h \cdot \mathbf{n}] \|_\ell$$

The above estimates in (41) yields the second estimate of (39). □

We now prove a result similar to lemma 2.3 in [19], see also theorem 3.2 in [6].

Lemma 7 *There is a constant C depending only on the shape of the mesh triangles such that, there are two functions v, w in $L^2(0, T; H^1(\Omega))$ satisfying,*

for all $K \in \mathcal{T}_h$

$$
\begin{aligned}
&\bullet\ |K|^2 \left(\Pi_K \left(\frac{\partial \phi_h}{\partial t} - \varepsilon^2 \Delta \phi_h - F_1(\phi_h) - c_h F_2(\phi_h) \right) \right)^2 \\
&\qquad = \int_K \Pi_K \left(\frac{\partial \phi_h}{\partial t} - \varepsilon^2 \Delta \phi_h - F_1(\phi_h) - c_h F_2(\phi_h) \right) v, \\
&\bullet\ \sum_{\ell \in E_K} |\ell|^2 \left(\varepsilon^2 \left[\nabla \phi_h \cdot \mathbf{n} \right] \right)^2 = \sum_{\ell \in E_K} \int_\ell \varepsilon^2 \left[\nabla \phi_h \cdot \mathbf{n} \right] v, \\
&\bullet\ |K|^2 \left(\Pi_K \left(\frac{\partial c_h}{\partial t} - D_1 \Delta c_h - div\ (D_2(c_h, \phi_h) \nabla \phi_h) \right) \right)^2 \\
&\qquad = \int_K \Pi_K \left(\frac{\partial c_h}{\partial t} - D_1 \Delta c_h - div\ (D_2(c_h, \phi_h) \nabla \phi_h) \right) w, \\
&\bullet\ \sum_{\ell \in E_K} |\ell|^2 \left[\left(D_1 \nabla c_h + \Pi_\ell (D_2(c_h, \phi_h) \nabla \phi_h) \right) \cdot \mathbf{n} \right]^2 \\
&\qquad = \sum_{\ell \in E_K} \int_\ell \left[\left(D_1 \nabla c_h + \Pi_\ell (D_2(c_h, \phi_h) \nabla \phi_h) \right) \cdot \mathbf{n} \right] w, \\
&\bullet\ \|v\|_K \leq C |K|^{1/2} \tilde{\eta}_K, \quad \|w\|_K \leq C |K|^{1/2} \tilde{\mu}_K, \\
&\bullet\ \|\nabla v\|_K \leq C \tilde{\eta}_K, \quad \|\nabla w\|_K \leq C \tilde{\mu}_K.
\end{aligned}
\tag{43}
$$

PROOF. We proceed as in [6,5,19] and choose, for all $(x,t) \in K \times (0,T)$:

$$
\begin{aligned}
v(x,t) &= C_0(t) \psi_K(x) + \sum_{i=1}^{3} C_i(t) \psi_{\ell_i}(x), \\
w(x,t) &= D_0(t) \psi_K(x) + \sum_{i=1}^{3} D_i(t) \psi_{\ell_i}(x),
\end{aligned}
$$

where ψ_K is the usual bubble function attached to K and ψ_{ℓ_i} is the bubble function attached to edge ℓ_i, $i = 1, 2, 3$. Inserting the above expressions for v and w in the second and fourth equation of (43), we obtain

$$
\begin{aligned}
C_i &= \frac{|\ell_i|^2 \varepsilon^2 \left[\nabla \phi_h \cdot \mathbf{n} \right]}{\int_{\ell_i} \psi_{\ell_i}} \\
D_i &= \frac{|\ell_i|^2 \left[\left(D_1 \nabla c_h + \Pi_\ell (D_2(c_h, \phi_h) \nabla \phi_h) \right) \cdot \mathbf{n} \right]}{\int_{\ell_i} \psi_{\ell_i}},
\end{aligned}
$$

for $i = 1, 2, 3$. Then, the first and third equation of (43) yields

$$C_0 = \frac{|K|^2 \Pi_K \left(\dfrac{\partial \phi_h}{\partial t} - \varepsilon^2 \Delta \phi_h - F_1(\phi_h) - c_h F_2(\phi_h) \right) - \sum_{i=1}^3 C_i \int_K \psi_{\ell_i}(x)}{\int_K \psi_K},$$

$$D_0 = \frac{|K|^2 \Pi_K \left(\dfrac{\partial c_h}{\partial t} - D_1 \Delta c_h - \text{div } (D_2(c_h, \phi_h) \nabla \phi_h) \right) - \sum_{i=1}^3 D_i \int_K \psi_{\ell_i}(x)}{\int_K \psi_K}.$$

Using the properties of bubble functions, there is a constant C depending only on the mesh regularity such that

$$C_0^2 + C_i^2 \leq C \tilde{\eta}_K^2 \quad \text{and} \quad D_0^2 + D_i^2 \leq C \tilde{\mu}_K^2,$$

and we obtain the last two estimates of (43). □

We now prove that $\tilde{\eta}_K$ and $\tilde{\mu}_K$ are bounded by the error.

Lemma 8 *There are two constants C_1 and C_2 independent of h such that, for all $K \in \mathcal{T}_h$, we have*

$$\begin{aligned}
\sum_{K \in \mathcal{T}_h} \tilde{\eta}_K^2 &\leq C_1 \varepsilon^4 \|\nabla(\phi - \phi_h)\|^2 \\
&\quad + C_2 h^2 \left(\left\| \frac{\partial}{\partial t}(\phi - \phi_h) \right\|^2 + \|\phi - \phi_h\|^2 + \|c - c_h\|^2 \right) \\
&\quad + C_2 \sum_{K \in \mathcal{T}_h} h_K^4 \left\| \nabla \left(\frac{\partial \phi_h}{\partial t} - \varepsilon^2 \Delta \phi_h - F_1(\phi_h) - c_h F_2(\phi_h) \right) \right\|_K^2, \\
\sum_{K \in \mathcal{T}_h} \tilde{\mu}_K^2 &\leq C_1 D_1^2 \|\nabla(c - c_h)\|^2 + C_1 \|D_2\|_{L^\infty(\mathbb{R}^2)}^2 \|\nabla(\phi - \phi_h)\|^2 \\
&\quad + C_2 \left(\|\phi_h - \phi\|^2 + \|c_h - c\|^2 \right) \\
&\quad + C_2 h^2 \left\| \frac{\partial}{\partial t}(c - c_h) \right\|^2 \\
&\quad + C_2 \sum_{K \in \mathcal{T}_h} h_K^4 \left\| \nabla \left(\frac{\partial c_h}{\partial t} - D_1 \Delta c_h - div \ (D_2(c_h, \phi_h) \nabla \phi_h) \right) \right\|_K^2 \\
&\quad + C_2 \sum_{K \in \mathcal{T}_h} \sum_{\ell \in E_K} |\ell|^3 \, \| [\nabla (D_2(c_h, \phi_h) \nabla \phi_h \cdot \mathbf{n})] \|_\ell^2 .
\end{aligned} \tag{44}$$

Moreover, C_1 depends only on the shape of the mesh triangles.

PROOF. We only prove the first estimate of (44), the second being obtained in the same manner. Using the results in Lemma 7, there is a function $v \in$

$L^2(0,T;H^1(\Omega))$ such that

$$\tilde{\eta}_K^2 = \int_K \left(\frac{\partial \phi_h}{\partial t} - \varepsilon^2 \Delta \phi_h - F_1(\phi_h) - c_h F_2(\phi_h) \right) v + \frac{1}{2} \sum_{\ell \in E_K} \int_\ell \varepsilon^2 \left[\nabla \phi_h \cdot \mathbf{n} \right] v + \delta_K(\phi_h, c_h),$$

where $\delta_K(\phi_h, c_h)$ is defined by

$$\begin{aligned} \delta_K(\phi_h, c_h) &= -\int_K (I - \Pi_K) \left(\frac{\partial \phi_h}{\partial t} - \varepsilon^2 \Delta \phi_h - F_1(\phi_h) - c_h F_2(\phi_h) \right) v \\ &= -\int_K (I - \Pi_K) \left(\frac{\partial \phi_h}{\partial t} - \varepsilon^2 \Delta \phi_h - F_1(\phi_h) - c_h F_2(\phi_h) \right) (I - \Pi_K) v. \end{aligned}$$

Integrating by parts and summing over the triangles, we have

$$\sum_{K \in \mathcal{T}_h} \tilde{\eta}_K^2 = \sum_{K \in \mathcal{T}_h} \int_K \left(\frac{\partial \phi_h}{\partial t} v + \varepsilon^2 \nabla \phi_h \cdot \nabla v - F_1(\phi_h) v - c_h F_2(\phi_h) v \right) + \sum_{K \in \mathcal{T}_h} \delta_K(\phi_h, c_h).$$

Using the weak form of (1), we then have

$$\begin{aligned} \sum_{K \in \mathcal{T}_h} \tilde{\eta}_K^2 = \sum_{K \in \mathcal{T}_h} \int_K \Bigg(& \frac{\partial}{\partial t}(\phi_h - \phi) v + \varepsilon^2 \nabla (\phi_h - \phi) \cdot \nabla v \\ & - (F_1(\phi_h) - F_1(\phi)) v - (c_h F_2(\phi_h) - c F_2(\phi)) v \Bigg) + \sum_{K \in \mathcal{T}_h} \delta_K(\phi_h, c_h). \end{aligned}$$

Using Cauchy-Schwarz inequality, the fact that F_1 and F_2 are smooth bounded functions, and that $0 \le c(x,t) \le 1$, there is a constant C independent of h such that

$$\begin{aligned} \sum_{K \in \mathcal{T}_h} \tilde{\eta}_K^2 \le \varepsilon^2 \sum_{K \in \mathcal{T}_h} \|\nabla(\phi_h - \phi)\|_K \, \|\nabla v\|_K + \sum_{K \in \mathcal{T}_h} \Bigg(& \left\| \frac{\partial}{\partial t}(\phi_h - \phi) \right\|_K \\ & + C \|\phi - \phi_h\|_K + C \|c - c_h\|_K \Bigg) \|v\|_K + \sum_{K \in \mathcal{T}_h} \delta_K(\phi_h, c_h). \end{aligned}$$

From standard interpolation properties of Π_K, there is a constant C depending only the on the shape of the mesh triangles such that

$$\delta_K(\phi_h, c_h) \le C h_K^2 \left\| \nabla \left(\frac{\partial \phi_h}{\partial t} - \varepsilon^2 \Delta \phi_h - F_1(\phi_h) - c_h F_2(\phi_h) \right) \right\|_K \|\nabla v\|_K.$$

Using the last two estimates of (43) in the two above estimates together with Young's inequality yields the first estimate of (44). □

Before stating the main results of this section, we need a convergence assumption similar to (15) and strong stability assumptions. We assume that there are two constant $C > 0$ and $s \in]0,1]$ independent of h such that

$$
\begin{aligned}
&\bullet \int_0^T \left(\left\| \frac{\partial}{\partial t}(\phi - \phi_h) \right\|^2 + \left\| \frac{\partial}{\partial t}(c - c_h) \right\|^2 \right) \\
&\qquad \leq C h^{2s} \int_0^T \Big(\|\nabla(\phi - \phi_h)\|^2 + \|\nabla(c - c_h)\|^2 \Big), \\
&\bullet \int_0^T \sum_{K \in \mathcal{T}_h} h_K^3 \left\| \nabla \left(\frac{\partial \phi_h}{\partial t} - \varepsilon^2 \Delta \phi_h - F_1(\phi_h) - c_h F_2(\phi_h) \right) \right\|_K \\
&\qquad \left\| \frac{\partial \phi_h}{\partial t} - \varepsilon^2 \Delta \phi_h - F_1(\phi_h) - c_h F_2(\phi_h) \right\|_K \leq C h^{2+s}, \\
&\bullet \int_0^T \sum_{K \in \mathcal{T}_h} h_K^4 \left\| \nabla \left(\frac{\partial \phi_h}{\partial t} - \varepsilon^2 \Delta \phi_h - F_1(\phi_h) - c_h F_2(\phi_h) \right) \right\|_K^2 \leq C h^{2+s}, \\
&\bullet \int_0^T \sum_{K \in \mathcal{T}_h} h_K^3 \left\| \nabla \left(\frac{\partial c_h}{\partial t} - D_1 \Delta c_h - \text{div } (D_2(c_h, \phi_h) \nabla \phi_h \right) \right\|_K \\
&\qquad \left\| \frac{\partial c_h}{\partial t} - D_1 \Delta c_h - \text{div } (D_2(c_h, \phi_h) \nabla \phi_h \right\|_K \leq C h^{2+s}, \\
&\bullet \int_0^T \sum_{K \in \mathcal{T}_h} h_K^4 \left\| \nabla \left(\frac{\partial c_h}{\partial t} - D_1 \Delta c_h - \text{div } (D_2(c_h, \phi_h) \nabla \phi_h \right) \right\|_K^2 \leq C h^{2+s}, \\
&\bullet \int_0^T \sum_{K \in \mathcal{T}_h} \sum_{\ell \in E_K} |\ell|^2 \, \| [\nabla (D_2(c_h, \phi_h) \nabla \phi_h \cdot \mathbf{n})] \|_\ell \, \| [D_2(c_h, \phi_h) \nabla \phi_h \cdot \mathbf{n}] \|_\ell \leq C h^{2+s}, \\
&\bullet \int_0^T \sum_{K \in \mathcal{T}_h} \sum_{\ell \in E_K} |\ell|^3 \, \| [\nabla (D_2(c_h, \phi_h) \nabla \phi_h \cdot \mathbf{n})] \|_\ell^2 \leq C h^{2+s}.
\end{aligned}
\tag{45}
$$

With the above assumptions we can now prove the following theorem.

Theorem 9 *Assume that (15) and (45) hold. Let ϕ, c be the solution of (8) (9), let ϕ_h, c_h be the solution of (13) (14) and let η_K^2, μ_K^2 be defined by (28) (29). Finally, let M_2 be defined by $M_2 = \|D_2\|_{L^\infty(\mathbb{R}^2)}$. Then, there are two constants C_1 and C_2 independent of h such that, for h sufficiently small, we have*

$$
\begin{aligned}
&\frac{1}{\varepsilon^2} \int_0^T \sum_{K \in \mathcal{T}_h} \eta_K^2 + \frac{\varepsilon^2}{M_2^2} \int_0^T \sum_{K \in \mathcal{T}_h} \mu_K^2 \\
&\leq C_1 \left(\varepsilon^2 \int_0^T \|\nabla(\phi - \phi_h)\|^2 + \frac{\varepsilon^2 D_1^2}{M_2^2} \int_0^T \|\nabla(c - c_h)\|^2 \right) + C_2 h^{2+s}.
\end{aligned}
\tag{46}
$$

Moreover, C_1 depends only on the shape of the mesh triangles.

PROOF. For each $K \in \mathcal{T}_h$, we consider the term

$$\frac{1}{\varepsilon^2}\eta_K^2 + \frac{\varepsilon^2}{M_2^2}\mu_K^2,$$

use Lemma 6 and 8, sum over $K \in \mathcal{T}_h$, integrate between $t = 0$ and $t = T$, use the assumptions (15) and (45), and obtain the result for h small enough.

Remark 10 *Let us discuss assumptions (45). Assumption one is, to some extend, similar to (15). This assumption is valid for instance when the error in the $H^1(0,T;L^2(\Omega))$ is bounded by a constant times h^2 (this result is available in Theorem 6.3 of [34] for the heat equation, for sufficiently large times and provided the solution is smooth) and when the error in the $L^2(0,T;H^1(\Omega))$ norm is greater than a constant times h (see Remark 1). Assumptions two to five hold whenever stability estimates can be proved on $\nabla\frac{\partial\phi_h}{\partial t}$ and $\nabla\frac{\partial c_h}{\partial t}$ (note that the use of an inverse estimate is not sufficient). The last two assumptions require even stronger stability estimates. Proving all these stability estimates is not an obvious task and is beyond the scope of the present paper.*

6 Numerical study of the effectivity index

In the sequel, we check that our error estimates are sharp for a realistic test case and propose a numerical study of the effectivity index. Before testing the quality of our error estimator, we propose a time discretization for solving (13) (14). Let J be the number of vertices of the triangulation $\mathcal{T}_h$, let $\varphi_1, \varphi_2, ..., \varphi_J$ be the usual hat functions corresponding to the vertices $P_1, P_2, ..., P_J$, we have :

$$\phi_h(x,t) = \sum_{j=1}^{J} \phi_j(t)\varphi_j(x), \qquad c_h(x,t) = \sum_{j=1}^{J} c_j(t)\varphi_j(x),$$

for all $x \in \bar{\Omega}$, $t \in (0,T)$. The differential system corresponding to (13) (14) then writes

$$\begin{aligned} M\dot{\vec{\phi}}(t) + \varepsilon^2 A\vec{\phi}(t) &= \vec{F}(\vec{\phi}(t), \vec{c}(t)), \\ M\dot{\vec{c}}(t) + D_1 A\vec{c}(t) &= D(\vec{\phi}(t), \vec{c}(t))\vec{\phi}(t). \end{aligned}$$

Here $\vec{\phi}(t)$ and $\vec{c}(t)$ are the vector of components $\phi_j(t)$, $c_j(t)$, respectively; M, A are the usual mass and stiffness matrices, respectively; $\vec{F}$ is the vector containing the nonlinears terms of (13) and $D(\vec{\phi}(t), \vec{c}(t))$ is the matrix corresponding to the nonlinear term of (14), namely :

$$D_{ij}(\vec{\phi}(t), \vec{c}(t)) = \int_\Omega D_2(c_h(t), \phi_h(t))\nabla\varphi_i \cdot \nabla\varphi_j,$$

for $i, j = 1, 2, ..., J$. In order to solve this nonlinear differential system, the following semi-implicit time discretization is considered. Let N be the number of time steps, $\tau = T/N$ the time step, $t_n = n\tau$, $n = 0, 1, ..., N$. Let $\vec{\phi}^n$, $\vec{c}^n$ be approximations of $\vec{\phi}(t_n)$ and $\vec{c}(t_n)$, $n = 0, 1, ..., N$. At each time step, we then solve successively the two following linear systems :

$$M\frac{\vec{\phi}^{n+1} - \vec{\phi}^n}{\tau} + \varepsilon^2 A\vec{\phi}^{n+1} = \vec{F}(\vec{\phi}^n, \vec{c}^n),$$
$$M\frac{\vec{c}^{n+1} - \vec{c}^n}{\tau} + D_1 A\vec{c}^{n+1} = \vec{D}(\vec{\phi}^{n+1}, \vec{c}^n)\vec{\phi}^{n+1}.$$

Thus, at each time step, two linear systems are to be solved in order to obtain $\vec{\phi}^n$ and $\vec{c}^n$. According to [25], this scheme is convergent, the error in the $L^\infty(0, T; L^2(\Omega))$ discrete norm is $O(h^2 + \tau)$, the error in the $L^2(0, T; H^1(\Omega))$ discrete norm is $O(h + \tau)$. We could proceed in the same manner to prove similar results for the semi-discrete problem (13) (14).

In order to test the quality of our error estimator, we consider a test case for which the exact solution to the problem (1)-(4) is known explicitly. For this purpose we choose Ω to be a square with side $\ell = 3.6\ 10^{-6}$, we set the final time $T = 10^{-5}$ and we add right hand sides to equations (1) (2) and compute them so that ϕ and c are given by

$$\begin{aligned}
\phi(x,t) &= 0.0 && \text{if } r(x) - vt - R_0 \leq -\delta,\\
&= \exp\left(\frac{\left(\frac{r(x) - vt - R_0}{\delta}\right)^2}{\left(\frac{r(x) - vt - R_0}{\delta}\right)^2 - 1}\right) && \text{if } -\delta < r(x) - vt - R_0 < 0,\\
&= 1.0 && \text{else,}
\end{aligned}$$

and $c(x,t) = 0.25 + 0.5\phi(x,t)$. Here $r(x)$ is the distance to the center of the square Ω, $v = 0.1$, $R_0 = 6\ 10^{-7}$ and $\delta = 5\ 10^{-7}$. Thus the isovalues of the solution are expanding circles centered on Ω, with a boundary layer of width δ. The physical data corresponding to the parameters introduced in section 2 are reported in table 1. The polynomials g and p are defined by $g(\phi) = \phi^2(1 - \phi^2)$ and $p(\phi) = \phi^3(6\phi^2 - 15\phi^4 + 10)$.

ε^2	M_ϕ	D_1	θ	v_m	R
10^{-9}	$4.948\ 10^{-3}$	10^{-9}	1573	$7.4\ 10^{-6}$	8.314
L^A	L^B	θ_m^A	θ_m^B	W^A	W^B
$2.35\ 10^9$	$1.725\ 10^9$	1728	1358	$1.11\ 10^7$	$6.357\ 10^6$

Table 1
Values of the physical parameters introduced in section 2.

In order to avoid the error due to time discretization we select a very small time step $\tau = 5\ 10^{-9}$ (thus the number of time steps is $N = 2000$). We consider uniform meshes of Ω into triangles such that h/ℓ (the ratio between the triangles sides and the size of the calculation domain Ω) goes to zero. In fig. 2, we have reported the error $\phi - \phi_h$ and $c - c_h$ in the $L^2(0,T;L^2(\Omega))$ and $L^2(0,T;H^1(\Omega))$ norms. Clearly the errors in the $L^2(0,T;L^2(\Omega))$ norm is $O(h^2)$ and the error in the $L^2(0,T;H^1(\Omega))$ norm is $O(h)$ which is consistent with assumption (15) and with the theoretical predictions obtained in [25].

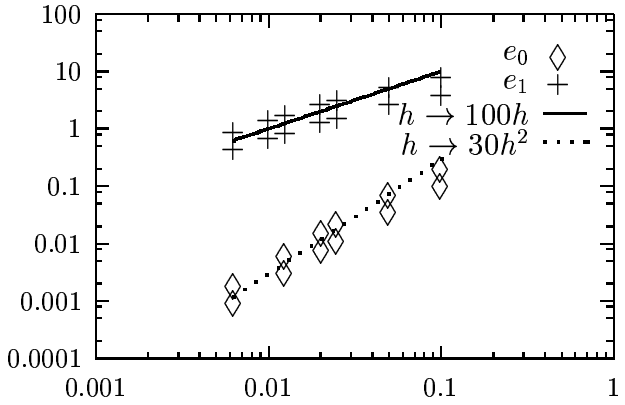

Fig. 2. Error $\phi - \phi_h$ and $c - c_h$ in the $L^2(0,T;L^2(\Omega))$ norm (e_0, lozanges) and $L^2(0,T;H^1(\Omega))$ norm (e_1, crosses) with respect to h.

From the theoretical results of section 4 and 5, we know that the error in the $L^2(0,T;H^1(\Omega))$ norm is bounded above and below by some error estimator, this being a classical result for elliptic problems [6,5,12] and linear parabolic problems [17,19]. In order to test the quality of our error estimator we define the two concentration effectivity indices eff_ϕ and eff_c by

$$\mathrm{eff}_\phi = \frac{\dfrac{1}{\varepsilon^2}\left(\displaystyle\int_0^T \sum_{K\in\mathcal{T}_h} \eta_K^2\right)^{1/2}}{\left(\displaystyle\int_0^T \|\nabla(\phi-\phi_h)\|^2\right)^{1/2}}, \qquad \mathrm{eff}_c = \frac{\dfrac{1}{D_1}\left(\displaystyle\int_0^T \sum_{K\in\mathcal{T}_h} \mu_K^2\right)^{1/2}}{\left(\displaystyle\int_0^T \|\nabla(c-c_h)\|^2\right)^{1/2}},$$

where the local error estimators η_K and μ_K are defined in (28) (29). In fig. 3 we have plotted the two effectivity indices with respect to the number of vertices J (h goes to zero when J goes to infinity), Clearly, when h goes to zero, then the effectivity indices goes to a constant value close to 4, which shows that our error estimators are good numerical representations of the true errors. This value close to 4 has already been obtained experimentally by one of the authors in ref. [21] for a Laplace problem and a nonlinear diffusion-convection problem. From the theoretical point of view, in ref. [4,21] it is proved that the effectivity index for a Laplace problem and a nonlinear diffusion-convection problem does only depend on interpolation constants (thus on the shape of the triangles), for h sufficiently small. A sharp estimate of the effectivity index is also proposed in ref. [4] for uniform meshes and the value of 4 is within this estimate.

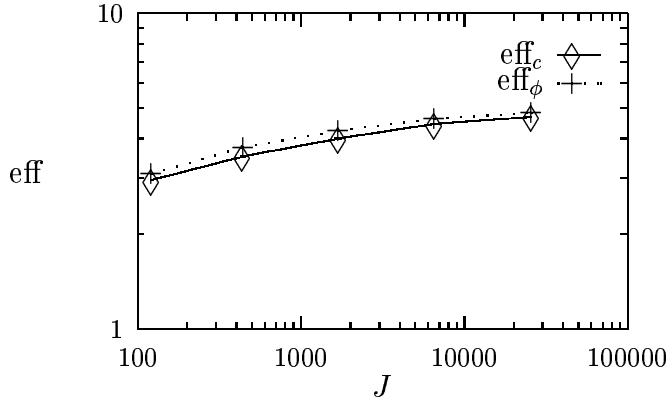

Fig. 3. Effectivity index with respect to the number of vertices when using uniform meshes.

Finally, we have reported in fig. 4 the local error $c - c_h$ at final time in the H^1 norm and the estimator μ_K as a function of the distance $r(x)$ to the center of the calculation domain Ω. Clearly, our error estimator is locally a good representation of the true error.

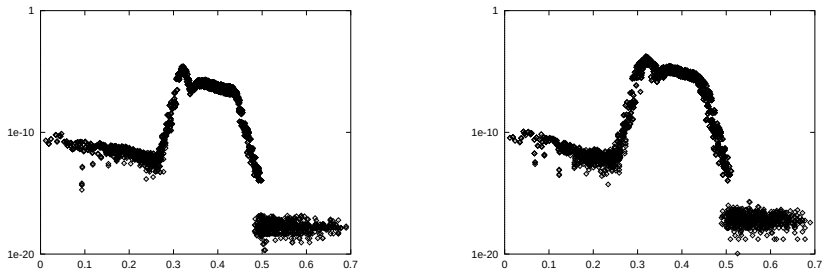

Fig. 4. True error ($\|\nabla(c - c_h)\|_K^2$, left fig.) and estimated error (μ_K^2, right fig.) at final time with respect to the normalized distance to the center of Ω ($r(x)/\ell$), when using uniform meshes.

7 An adaptive algorithm

In this section we present an adaptive algorithm based on the error estimator studied in section 4 and 5. This adaptive algorithm is first validated using the same test case as in section 6. Then, this adaptive algorithm is used to simulate the formation of solutal dendrites, as in [22].

The goal of our adaptive algorithm is, given a time step $\tau = T/N$, to build a sequence of triangulations $\tau_h^1, \tau_h^2, ..., \tau_h^N$ such that the estimated relative error is close to a preset tolerance TOL, namely :

$$0.5 \text{ TOL} \leq \frac{\frac{1}{D_1}\left(\int_0^T \sum_{K \in \mathcal{T}_h} \tilde{\mu}_K^2\right)^{1/2}}{\left(\int_0^T \|\nabla c_h\|^2\right)^{1/2}} \leq 1.5 \text{ TOL}. \tag{47}$$

Here $\tilde{\mu}_K$ is the modified estimator corresponding to the interelement jumps in μ_K, that is

$$\tilde{\mu}_K^2 = \frac{1}{2} \sum_{\ell \in E_K} |\ell| \left\| \left[\left(D_1 \nabla c_h + D_2(c_h, \phi_h) \nabla \phi_h \right) \cdot \mathbf{n} \right] \right\|_\ell^2 .$$

The reader should note that we have considered only the error estimator for the solute concentration c, the reason being the following. When computing solutal dendrites, both ϕ and c vary strongly in a small region corresponding to the solid-liquid interface. However, the function c may also vary in other regions, whereas ϕ does not, see Fig. 5.

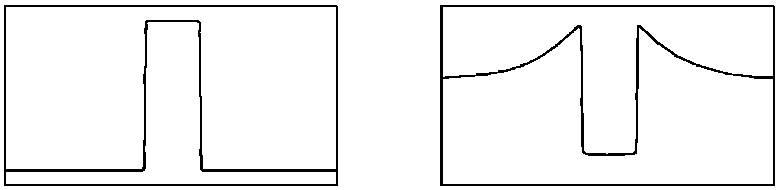

Fig. 5. Typical profiles of the phase field (left) and concentration field (right). The phase field has values zero or one, except in the phase change region. The concentration field changes rapidly across the phase change region, but may also vary outside the phase change region.

From the numerical experiments of the previous section, we have checked that both error estimators η_K and μ_K are good approximation of the true error (up to a factor close to 4). Thus, if we achieve (47), we hope to control the true

relative error

$$\frac{\left(\int_0^T \|\nabla c - c_h\|^2\right)^{1/2}}{\left(\int_0^T \|\nabla c_h\|^2\right)^{1/2}}.$$

A simple way to achieve (47) is , for all $n = 1, 2, ..., N$, to find a triangulation $\mathcal{T}_h^n$ such that the following inequalities hold :

$$0.5^2 \text{ TOL}^2 \int_{t_{n-1}}^{t_n} \|\nabla c_h\|^2 \leq \frac{1}{D_1^2} \int_{t_{n-1}}^{t_n} \sum_{K \in \mathcal{T}_h} \tilde{\mu}_K^2 \leq 1.5^2 \text{ TOL}^2 \int_{t_{n-1}}^{t_n} \|\nabla c_h\|^2.$$

We then proceed as in [35,19] to build the new triangulation. More precisely, if the above inequalities are satisfied, we go to the next time step. If the above inequalities are not satisfied, we refine or coarsen the mesh in order to equidistribute the local error estimator. Vertices are added or removed and a Delaunay triangulation is generated. The process is repeated until the above inequalities are satisfied.

As in fig. 3, we have plotted in fig. 6 the effectivity index with respect to the average number of vertices, when using our adaptive algorithm with several values of TOL. Clearly, the effectivity index goes to a constant value which is again close to 4.

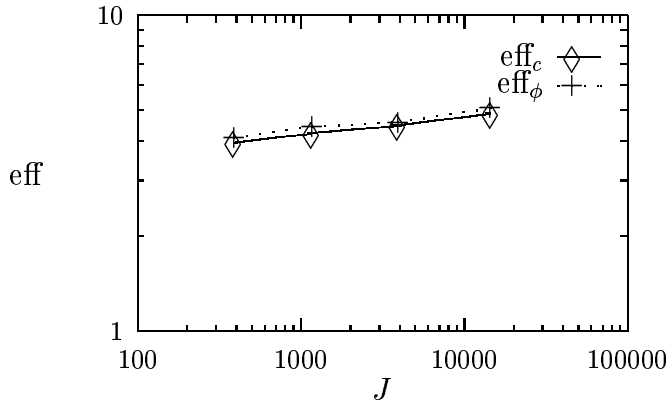

Fig. 6. Effectivity index with respect to the average number of vertices when using adapted meshes ($TOL = 1$, 0.5, 0.25, and 0.125).

In order to check the efficiency of our algorithm, we have plotted in fig. 7 the true error with respect to the average number of vertices J, when using both uniform and adapted triangulations. The average number of vertices required to reach a given level of accuracy is much lower when using adapted meshes.

As in fig. 4, we have reported in fig. 8 the local true and estimated errors with respect to the distance to the center of Ω. Clearly, the estimated error is equidistributed over the calculation domain.

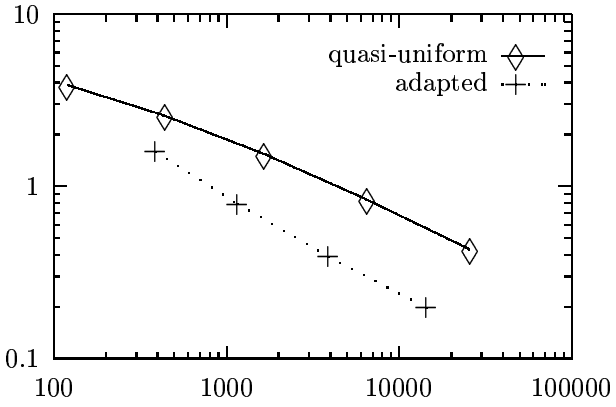

Fig. 7. Error $c - c_h$ in the $L^2(0,T;H^1(\Omega))$ norm with respect to the average number of vertices, when using uniform meshes and adapted meshes.

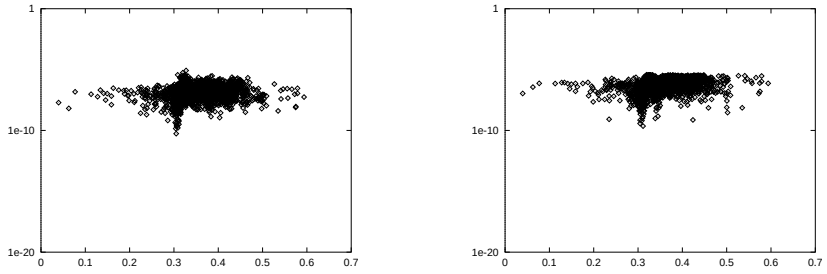

Fig. 8. True error ($\|\nabla(c - c_h)\|_K^2$, left fig.) and estimated error (η_K^2, right fig.) at final time with respect to the normalized distance to the center of Ω ($r(x)/\ell$), when using adapted meshes.

Finally, we have used our adaptive algorithm in order to simulate the growth of an isothermal solutal dendrite. In order to take into account anisotropic phenomena, we proceed as in [22] and modify the term $\tilde{\varepsilon}^2|\nabla\phi(x,t)|^2$ in (6) by $\tilde{\varepsilon}^2 a^2(\psi)|\nabla\phi(x,t)|^2$, where

$$a(\psi) = 1 + \bar{a}\,\cos(4\psi),$$

and where ψ denotes the angle between $\nabla\phi$ and the horizontal axis. Here $\bar{a}$ is the anisotropy coefficient, typical values being 0.02-0.05.

Introducing the anisotropy would obviously change the error indicators. However, from the theoretical point of view, the anisotropic model is not an obvious extension of the isotropic one, due to the fact that the diffusion operator becomes strongly nonlinear, see [36]. More precisely, existence and uniqueness can be proved for sufficiently small values of $\bar{a}$, namely $\bar{a} < \frac{1}{15}$.

Therefore, we have also used $\tilde{\mu}_K$ as an error indicator for the anisotropic case.

We take the same physical parameters than those of section 6 and choose $\bar{a} = 0.02$. At initial time, we place a small solid region of radius 2.10^{-7} at the center of the calculation domain Ω (the side is now $\ell = 3.6\ 10^{-5}$) with concentration 0.3994, whereas the liquid region has concentration 0.40831. For symmetry reasons, the computations are performed on quarter of the domain. The time step is $\tau = 2.\ 10^{-6}$, the preset tolerance is TOL= 0.5. In fig. 9, we have represented the adapted meshes, the concentration c and order parameter ϕ at several times. The computation took about 5 hours on a SGI R10000 250Mhz workstation.

From the physical point of view, dendrite formation is an unstable phenomena. From the numerical one, the results are very sensitive to the parameters used in the simulation. As an example, we have reported in fig. 10 the final shape of the dendrite obtained when setting the tolerance TOL to 0.5, 0.75 and 1. Clearly, when TOL is large, the solution is not precise since symmetry (which is a consequence of uniqueness) is not obtained. When TOL decreases, symmetry seems to be recovered (for memory reasons, we could not proceed with smaller values of TOL). Numerical results not reported here show that this numerical sensitivity increases when increasing M_ϕ (thus ε), this being coherent with classical results of physical stability.

Finally, it should be mentionned that an adaptive finite element method has been used (without theoretical justification) in [37] to simulate thermal dendrites.

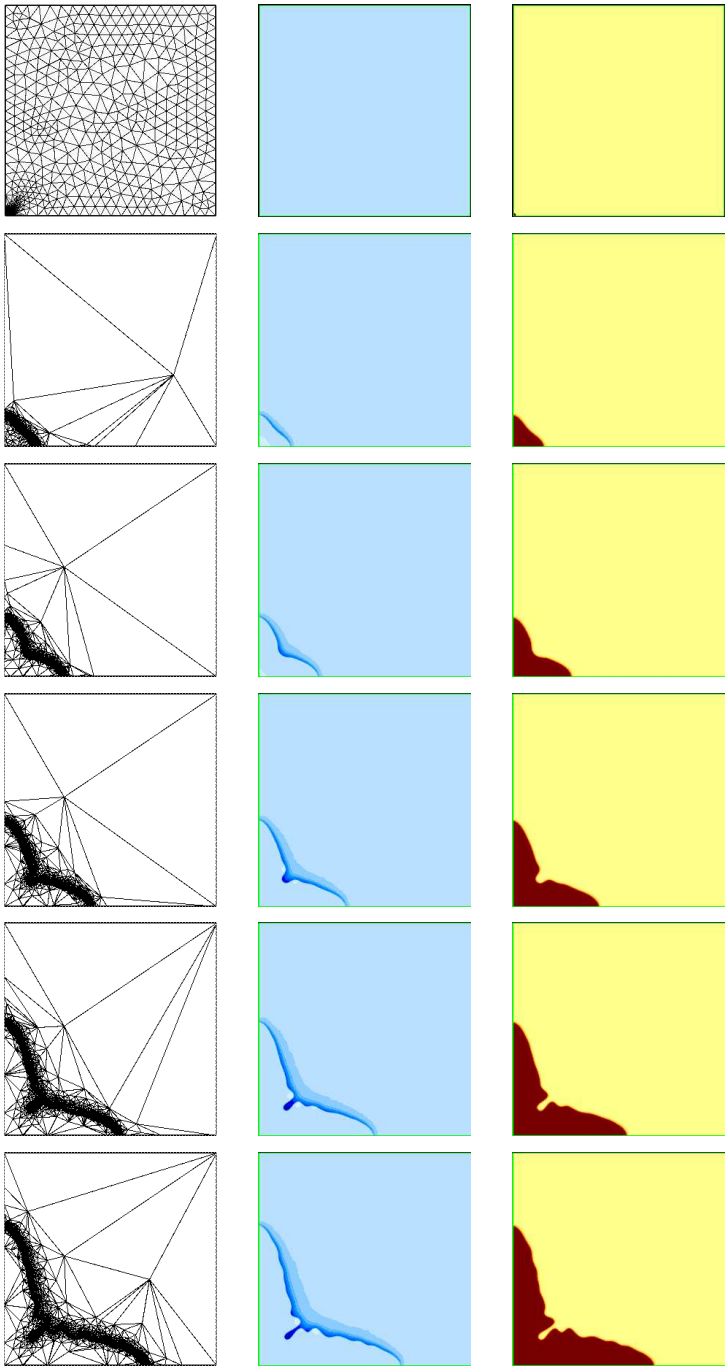

Fig. 9. Formation of a solutal dendrite. Adapted meshes (left col.), c isovalues (center col.), ϕ isovalues (right col.) at several times. First row : time 0, 3379 vertices; second row : time $2 \cdot 10^{-4}$, 4495 vertices; third row : time $4 \cdot 10^{-4}$, 7282 vertices; fourth row : time $6 \cdot 10^{-4}$, 10668 vertices; fifth row : time $8 \cdot 10^{-4}$, 14419 vertices; last row : time $1 \cdot 10^{-3}$, 18374 vertices.

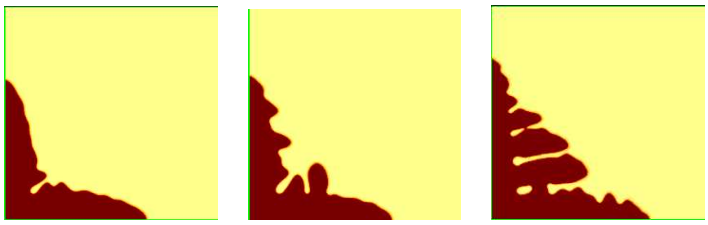

Fig. 10. Final shape of the dendrite with TOL=0.5, 0.75 and 1.

References

[1] I. Babuska and W.C. Rheinboldt. Error estimates for adaptive finite element computations. *SIAM J. Numer. Anal.*, 15:736–754, 1978.

[2] I. Babuska and W.C. Rheinboldt. A posteriori error estimators in the finite element method. *Internat. J. Numer. Meth. Engrg.*, 12:1597–1615, 1978.

[3] I. Babuska, T. Strouboulis, and C.S. Upadhyay. A model study of the quality of a posteriori estimators for linear elliptic problems. error estimation in the interior of patchwise uniform grids of triangles. *Comp. Meth. Appl. Mech. Eng.*, 114(4):307–378, 1994.

[4] M. Ainsworth and J.T. Oden. A unified approach to a posteriori error estimation using finite element residual methods. *Numer. Math.*, 65:23–50, 1993.

[5] R. Verfürth. A posteriori error estimators for the Stokes equations. *Numer. Math.*, 55:309–325, 1989.

[6] I. Babuska, R. Duran, and R. Rodriguez. Analysis of the efficiency of an a posteriori error estimator for linear triangular finite elements. *SIAM J. Numer. Anal.*, 29(4):947–964, 1992.

[7] C. Johnson. Adaptive finite element methods for diffusion and convection problems. *Comp. Methods Appl. Mech. Eng.*, 82:301–322, 1990.

[8] K. Eriksson and C. Johnson. Adaptive streamline diffusion finite element methods for stationary convection-diffusion problems. *Math. Comp.*, 60(201):167–188, 1993.

[9] J. Baranger and H. El-Amri. Estimateurs a posteriori d'erreur pour le calcul adaptatif d'écoulements quasi-newtoniens. *RAIRO M2AN*, 25(1):31–48, 1991.

[10] J. Pousin and J. Rappaz. Consistency, stability, a priori and a posteriori errors for Petrov-Galerkin methods applied to nonlinear problems. *Numer. Math.*, 69(2):213–232, 1994.

[11] G. Caloz and J. Rappaz. Numerical analysis for nonlinear and bifurcation problems. *to appear in Handbook of numerical analysis, P.G. Ciarlet and J.L. Lions Ed., North-Holland, Amsterdam*, 1997.

[12] R. Verfürth. A posteriori error estimates for nonlinear problems. finite element discretizations of elliptic equations. *Math. Comp.*, 62(206):445–475, 1994.

[13] K. Eriksson and C. Johnson. Adaptive finite element methods for parabolic problems I : a linear model problem. *SIAM J. Numer. Anal.*, 28(1):43–77, 1991.

[14] K. Eriksson and C. Johnson. Adaptive finite element methods for parabolic problems IV : nonlinear problems. Technical Report 44, Department of mathematics, Chalmers university of technology, the university of Göteborg, S-412 96 Göteborg, Sweden, 1992.

[15] R. H. Nochetto, G. Savaré, and C. Verdi. A posteriori error estimates for variable time-step discretizations of nonlinear evolution equations. *preprint*, 2000.

[16] R. H. Nochetto, A. Schmidt, and C. Verdi. A posteriori error estimation and adaptivity for degenerate parabolic problems. *Math. Comp., to appear*, 2000.

[17] R. Verfürth. A posteriori error estimates for nonlinear problems. finite element discretizations of parabolic equations. *Math. Comp.*, 67(224):1335–1360, 1998.

[18] R. Verfürth. A posteriori error estimates for nonlinear problems. finite element discretizations of parabolic equations. *Numer. Methods Partial Differential Equations*, 14(4):487–518, 1998.

[19] M. Picasso. Adaptive finite elements for a linear parabolic problem. *Comp. Meth. Appl. Mech. Eng.*, 167:223–237, 1998.

[20] S. Adjerid, J.E. Flaherty, and I. Babuska. A posteriori error estimation for the finite element method-of-lines solution of parabolic problems. *Math. Models Meth. Applied Sci.*, 9(2):261–286, 1999.

[21] S. Adjerid, B. Belguendouz, and J.E. Flaherty. A posteriori finite element error estimation for diffusion problems. *SIAM J. Sci. Comput.*, 21(2):728–746, 1999.

[22] J. A. Warren and W. J. Boettinger. Prediction of dendritic growth and microsegregation patterns in a binary alloy using the phase-field model. *Acta metall. mater.*, 43(2):689–703, 1995.

[23] J. Rappaz and J.-F. Scheid. Existence of solutions to a phase-field model for the isothermal solidification process of a binary alloy. *Math. Meth. Appl. Sci.*, 23:491–513, 2000.

[24] O. Kruger. *Modélisation et analyse numérique de problèmes de réaction-diffusion provenant de la solidification d'alliages binaires.* PhD thesis, Département de Mathématiques, Ecole Polytechnique Fédérale de Lausanne, 1999.

[25] D. Kessler and J.-F. Scheid. A priori error estimates for a phase-field model for the solidification process of a binary alloy. *IMA J. Numer. Anal.*, 22:281–305, 2002.

[26] D. Kessler, O. Kruger, and J.-F. Scheid. Construction d'un modèle de champ de phase. Technical report, Département de Mathématiques, Ecole Polytechnique Fédérale de Lausanne, 1015 Lausanne, Switzerland, 1999.

[27] J. Tiaden, B. Nestler, H. J. Diepers, and I. Steinbach. The multiphase-field model with an integrated concept for modelling solute diffusion. *Physica D: Nonlinear Phenomena*, 115(1-2):73–86, 1998.

[28] D. Kessler. Sharp interface limits of a thermodynamically consistent phase field model. *J. Crystal Growth*, 224:175–186, 2001.

[29] P.G. Ciarlet. *The Finite Element method for elliptic problems.* Academic Press, London, 1990.

[30] I. Babuška and A. Miller. A feedback finite element method with a posteriori error estimation. I. The finite element method and some basic properties of the a posteriori error estimator. *Comput. Methods Appl. Mech. Engrg.*, 61(1):1–40, 1987.

[31] J. Medina, M. Picasso, and J. Rappaz. Error estimates and adaptive finite elements for nonlinear diffusion-convection problems. *Math. Models Methods Appl. Sciences*, 6(5):689–712, 1996.

[32] D. Henry. *Geometric theory of semilinear parabolic equations.* Springer-Verlag, Berlin, 1981.

[33] P. Clément. Approximation by finite element functions using local regularization. *RAIRO Anal. Numér.*, 9:77–84, 1975.

[34] Vidar Thomée. *Galerkin finite element methods for parabolic problems.* Springer-Verlag, Berlin, 1997.

[35] M. Picasso. An adaptive finite element algorithm for a two-dimensional stationary stefan-like problem. *Comp. Meth. Appl. Mech. Eng.*, 124:213–230, 1995.

[36] E. Burman and J. Rappaz. Existence of solutions to an anisotropic phase-field model. Technical report, Département de Mathématiques, Ecole Polytechnique Fédérale de Lausanne, 1015 Lausanne, Switzerland, 2001.

[37] N. Provatasa, N. Goldenfeld, and J. Dantzig. Adaptive mesh refinement computation of solidification microstructures using dynamic data structures. *J. Comput. Phys.*, 148(1):265–290, 1999.